eprints@whiterose.ac.uk
https://eprints.whiterose.ac.uk/

Effects of Jatropha lubricant thermo-oxidation on the tribological behavior of engine cylinder liners as measured by a reciprocating friction test

[a] Leonardo Israel Farfan-Cabrera, [b] Ezequiel Alberto Gallardo-Hernández, [c] José Pérez-González, [d] Benjamín Marcos Marín-Santibáñez, [e] Roger Lewis

[a] *Tecnologico de Monterrey, Escuela de Ingeniería y Ciencias, Vía Atlixcáyotl No. 5718, Reserva Territorial Atlixcáyotl, 72453, Puebla, Puebla, México.*

[b] *Instituto Politécnico Nacional, SEPI-Escuela Superior de Ingeniería Mecánica y Eléctrica, Unidad Zacatenco, Grupo de Tribología, Col. Lindavista, C.P. 07738, Ciudad de México, México.*

[c] *Instituto Politécnico Nacional, Escuela Superior de Física y Matemáticas, Laboratorio de Reología y Física de la Materia Blanda, U.P. Adolfo López Mateos Edif. 9, Col. Lindavista, Ciudad de México, México.*

[d] *Instituto Politécnico Nacional, Escuela Superior de Ingeniería Química e Industrias Extractivas, U.P. Adolfo López Mateos Edif. 7, Col. Lindavista, Ciudad de México, México*

[e] *The University of Sheffield, Department of Mechanical Engineering, Sheffield, UK*

Abstract

Bio-lubricants have emerged as a potential and viable way to replace, totally or partially, mineral oils due to their effectiveness in the boundary lubrication regime for different applications, including, automotive engine operation. However, the effect of thermo-oxidation caused by the long-term use of the bio-lubricants on their tribological properties has been scarcely analyzed. In this work, the effect of thermo-oxidation of Jatropha oil (JO), an engine mineral oil (EMO) and a blend made up of 80%vol. EMO and 20%vol. JO (B20) on the tribological behavior of a simulated piston ring/engine cylinder liner interface was studied in reciprocating friction tests at 26 and 100°C. The oils were thermally oxidized and characterized in terms of carbonyl compounds, depletion of ZDDP additives, changes in kinematic viscosity and viscosity index. Friction coefficients, wear rates and scar morphologies were assessed. Thermo-oxidation resulted in significant viscosity increases in JO compared to EMO and B20. Also, it generated increased friction coefficients for JO and B20. However, they were lower than those for fresh and aged EMO. EMO increased the wear rate after thermo-oxidation in contrast to JO. Smearing was generated using most oil samples while severe scuffing was only produced by using fresh JO at 100°C.

Keywords

Internal combustion engines; Boundary lubrication; Thermal effects; Lubricated wear including scuffing; Bio-lubricant

1. Introduction

The piston assembly and cylinder liners are two of the most important components in a reciprocating internal combustion engine. These components allow the dynamic sealing of the combustion chamber through the piston reciprocating motion, which is the link to transform the energy generated by combustion into kinetic energy. The engine efficiency depends strongly on the dynamic sealing and friction performance of the piston assembly within cylinder liners. Poor sealing capacity results in decreased combustion efficiency meanwhile increased friction can generate rise of fuel consumption. According to Holmeberg et al. [1], a percentage between 4.3 and 7.8% of fuel energy is dissipated by the friction between the piston assembly and the cylinder liner. The friction generated by the piston assembly against cylinder liners represent around 45% of the total engine friction losses, followed by bearings, seals and other components operating under hydrodynamic lubrication regime (20-44%), the valve train (3-34%) and oil pumping and hydraulic viscous losses (10%). Thus, the former can be considered as the largest source of friction losses in engine. Advanced coatings and surface texturing have been suggested to reduce friction and wear. Besides, new lubricants and additives technologies with low-viscosity and low-shear are being developed [1].

The piston assembly operates under large and rapid variations of load, speed, temperature and lubricant feeding. So, the piston assembly may experience boundary, mixed and hydrodynamic film lubrication even in a single piston stroke [2]. In a recent approaching reported by Wong and Tung [3], it was claimed that the piston assembly mainly operates in the mixed lubrication regime when using low-viscosity oils. Nonetheless, boundary lubrication is expected at the top dead centre (TDC) and bottom dead centre (BDC) piston positions where the sliding speed reaches zero, limiting the formation of a mixed or hydrodynamic film. Mixed lubrication occurs at the transition from hydrodynamic to boundary lubrication situations and vice versa. The thermal expansion and wear of the cylinder liner cause sealing deficiency in the combustion chambers generating a reduction in the peak compression pressure and an increase in oil consumption [4].

Many efforts have been conducted to reduce friction and wear in reciprocating combustion engines. Nevertheless, it has been demonstrated that the use of energy-conserving engine lubricants is the most economical way to acquire the necessary gains [5]. The increasing demand for more efficient and ecofriendly engine lubricants has promoted interest in investigating the potential of bio-oils as engine lubricants. The tribological properties of different pure vegetable oils or mineral oil blends have been well investigated. Most bio-oils have been demonstrated to exhibit better lubricity properties than mineral oils when used in the boundary lubrication regime. This is attributable to the high proportion of free fatty acids they contain, which act as effective friction modifiers [6-11]. However, the confident total use of bio-oils as engine lubricants has not been authenticated since they exhibit poor oxidation stability and generate considerable high wear compared with mineral oils, which may damage engine components with their long-term use [9, 10, 12-15].

Usually, the ageing of engine oils is characterized by oxidation, additive depletion and neutralization of the oil. However, the thermal oxidative stability is the most important property to be considered because they have a great influence on changes in viscosity and viscosity index, density, and tribological properties [16, 17]. Engines work efficiently in the range between 90 and 100 °C under normal operation, so a good lubricant is required to show minimal degradation at these temperatures. The physical and chemical changes of oil due to thermal ageing impact on the lubrication performance [17]. In this regard, it is important to consider that vegetable oils have poor thermal oxidation stability due to their chemical composition conductive to faster degradation during their lifetime, either in storage or in use, than mineral oils [18].

The effects of thermo-oxidation of some bio-oils on their tribological performance have been investigated previously. Mannekote and Kailas [19] studied the effect of oxidation on the tribological performance of groundnut, palm, rice bran, soybean, and sesame oils. The oils were thermally aged by heating them at 60, 80 and 100 °C in a dark oven for 14, 28, and 42 days. Tribological tests were then conducted in a four-ball tester to determine changes in friction coefficients and wear in the boundary lubrication regime. The authors concluded that all oil samples exhibited increase in free fatty acids, peroxides, and viscosity. Besides, the wear increased with ageing time and temperature. Meanwhile the friction coefficients decreased for the oxidized oil samples due to tribo-chemical reactions (formation of iron soap on the metallic surfaces). Kreivaitis et al. [20] investigated the influence of oxidation on tribological properties of rapeseed oil using four-ball tribological tests. The oil sample was oxidized according to the standard method ISO 6886:2006 using Rancimat 743 apparatus. The oil was heated to 100 °C for various periods up to 40 h. The results suggested that oxidation time decreased lubricity of the oil. Thus, it can be concluded that bio-lubricants present better lubricity than mineral oils in a fresh state, but they may lose their tribological properties by oxidation.

Currently, Jatropha oil (JO) is considered as one of the most promising options as a bio-lubricant since it presents various advantages. The plant has a high oil content; it can grow on marginal lands in tropical and sub-tropical climates enabling an extensive oil source supply, and it is not considered as human feedstock [11, 21]. It has been demonstrated that JO exhibits better tribological properties than other bio-oils, for example, rapeseed oil [10] and is compatible with different sealing elastomers from fuel and lubrication systems [22, 23, 24]. It has also been reported that the frictional coefficients are reduced by blending JO with mineral oils for different applications, namely, hydraulic fluids [25], engine oils [14], metal working fluids [26, 27], automatic transmission fluids [28], drilling muds [29], etc. Negligible changes in terms of wear have been

reported by using low percentages (<20%) of JO in blends with mineral oils [14]. Overall, the literature suggest that JO could be blended in low percentages with engine oils and other lubricants to enhance their tribological performance.

Despite the extensive research mentioned above on tribological properties of JO, there is a dearth of information about the effect of thermo-oxidation resulting from storage and use on its tribological behavior. The aim of this work was to evaluate the tribological behavior of engine cylinder liners lubricated with fresh and thermo-oxidized JO using reciprocating tests, replicating severe sliding conditions in actual engine operation. For the purpose of comparison, an engine mineral oil (EMO) and a blend made of 80% vol. EMO and 20% vol. JO were also evaluated under the same experimental conditions. The oils were thermally oxidized by a laboratory method consisting of heating the lubricants at 160 °C for two different periods (30 and 60 h). The changes occurring in the oils in terms of carbonyl compounds, depletion of Zinc dialkyldithiophosphate (ZDDP) (for EMO and B20), density, viscosity and viscosity index were analyzed. Tribological tests were then carried out in a reciprocating friction tester using steel balls against samples extracted from actual engine cylinder liners made of gray cast iron and conditioned by plateau honey finishing.

2. Experimental details

2.1 Oil samples

The lubricants tested were JO (filtered and used without refining (straight JO)), an engine mineral oil (EMO) (SAE 10W-30 API SL), and a blend (B20) made up of 80%vol. of EMO and 20%vol. of JO. The fatty acid profile of the JO is given in Table 1. It was characterized by ESI mass spectroscopy analyses using a MALDI-TOF spectrometer (Bruker DHAP). To examine the thermal-oxidative stability of the oils, they were exposed to a laboratory artificial ageing process [30]. This has been demonstrated as a short-term method to investigate the long-term behavior of engine oils, enabling the pre-selection thereof according to their performance under special conditions. For this, 300 g of oil were heated for 30 and 60 h in a sealed beaker at 160±0.5 °C by using a stirring hotplate with temperature control. According to the method [30], the temperature corresponds to the value in which the main deterioration of the lubricant takes place in the combustion chamber. Air was introduced directly into the oil at a rate of 10 l/h to facilitate the oxidation process and accelerate degradation of the oil sample as suggested in the method [30]. It is noteworthy that actual ageing environments of engine oils involve interaction with other species in the combustion chamber, namely, fuel elements, exhaust gases, soot, etc., producing also sulfhonation, nitration, etc. Considering the different alternative fuels existing today, a more realistic approach incorporating these effects would involve much extensive further research work.

Table 1. Fatty acids profile of straight Jatropha oil (JO).

Fatty acid	Araquidic	Linoleic	Behenic	Oleic	Lauric
%	32.71	26.63	25.23	11.22	4.2

The oxidation characteristics of the oil samples were evaluated by using the standard method detailed in ASTM D-7214 which involves using Fourier transform infrared spectroscopy (FT-IR). It enables the measurement of the change in concentration of constituents containing a carbonyl function that have formed during the oxidation process. The method consists of recording the FT-IR spectra of the fresh and aged oils in a transmission cell of known pathlength. Both spectra are converted to absorbance, and then, subtracted. Using the differential spectrum, a baseline is set under the peak corresponding to the carbonyl region between 1650 and 1820 cm^{-1}. The area created by this baseline and the carbonyl peak is calculated and divided by the cell pathlength. The result is reported as peak area increase (PAI). The standard method ASTM D-7412 was used to monitor depletion of anti-wear additives (zinc dialkyldithiophosphate (ZDDP)) in EMO and B20 by

performing FT-IR analysis. The ZDDP concentration was calculated from each spectrum of the oil samples by the direct measurement of the area comprised between 960 and 1025 cm^{-1} using a baseline between 700 and 1900 cm^{-1}. Both analyses were conducted by using a spectrometer micro Raman (LabRam HR800) coupled to an ATR (objective 36X) from a module FT-IR (IR2). The cell pathlength was set at 0.05mm. The spectral data were collected between 700 and 1900 cm^{-1}, averaging 32 scans with a resolution of 4 cm^{-1}. The data range was selected to meet the required spectra in both ASTM methods.

The viscosity changes caused by thermo-oxidation were also evaluated. The dynamic viscosities were measured by using a rotational rheometer (TA Instruments/ARG2) with a cone/plate configuration at 26, 40 and 100 °C, respectively. Densities were obtained at the same set of temperatures to calculate the kinematic viscosities. In addition, the viscosity indexes were calculated by following the ASTM D-2270 standard procedure. All the tests were carried out for the fresh and thermo-oxidized oil samples.

2.2 Reciprocating friction test set-up

Tribological tests were carried out by using a friction reciprocating tester. A schematic view is shown in Fig. 1a. A steel ball specimen is clamped by the ball holder, which is fixed to the reciprocating arm. A cylinder liner sample is secured tightly into an oil bath permitting the free parallel movement of the reciprocating arm, as represented in Fig. 1b. A predefined normal load is applied to the ball holder. A force sensor is located and fixed next to the oil bath to measure the tangential force (friction force) generated by the reciprocating action of the ball against the cylinder liner specimen. An electrical resistance heater is located under the oil bath to rise and control the oil temperature. Temperature is monitored through the entire test by means of a thermocouple immersed in the oil. The ball samples were commercial steel balls (alloy 1018) with a 6 mm diameter and 0.02 µm roughness (Ra). The cylinder liner specimens were prepared with dimensions of 30 x 20 mm. They were cut from actual cylinder liners (78 mm in diameter and 3 mm in thickness) made of gray cast iron with surface conditioning by plateau honing process. The specimens were characterized to obtain the values of hardness, elastic modulus and roughness, which are given in Table 2. The hardness and elastic modulus were measured by Berkovich nanoindentation tests on the cross-section of the samples meanwhile the surface roughness was measured in terms of Sa and Sq parameters using an optical profilometer. The elemental composition of the samples is given in Table 3. It was obtained by an energy dispersive spectroscopy (EDS) analysis.
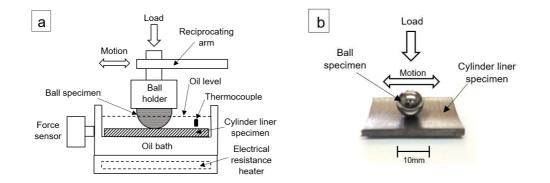

Figure 1. a) Schematic representation of the reciprocating friction test set-up; b) steel ball and cylinder liner specimens.

Table 2. Mechanical properties of the steel ball and cylinder liner specimens.

Sample	Hardness (HV)	Elastic modulus (GPa)	Roughness (µm)
Steel ball (alloy 1018)	760-840	207	Ra=0.02

Grey cast iron liner	428.6±59.5	95.7±5.8	Sa=1.135; Sq=1.51

Table 3. Elemental composition of cylinder liner specimens.

Sample	Chemical composition			
	Fe (%)	C (%)	O (%)	Si (%)
Cylinder liner (grey cast iron)	66.1±4.56	17.2±4.23	13.6±2.35	3.1±1.25

2.3 Tribological test conditions

The test conditions are given in Table 4. Two different oil temperatures (26 and 100 °C) were tested since they are representative of internal combustion engines operation. 26 °C can be considered as the average temperature when the engine is started meanwhile 100 °C may be considered as the mean temperature when the engine is running steadily. The load, the reciprocating frequency and duration of test were characteristic conditions of the actual contact when there is a severe sliding condition occurring in the piston rings/cylinder liner interface under a boundary lubrication regime. According to the configuration of a ball on a concave surface, the contact pressure was estimated by the solution given by Johnson for elastic elliptical contacts [31]. The stroke length of the tester was adjusted to 12 mm to generate measurable wear scars. For each test, 10 ml of oil was poured into the oil bath to ensure full immersion of the contact for the entire test. Four similar experiments were conducted for each set of test conditions. The friction force was monitored and logged via data acquisition software for the entire test. The morphology and topography of the wear scars were evaluated using an electron scanning microscope (SEM) and an optical profilometer to visualize the wear features and to measure the wear volumes, respectively. The test duration and load were selected to obtain stable friction and measurable scars on all the samples. Several previous trials were conducted to determine these parameters. Three regions in the friction progression for 25 minutes were identified. The first stage is the well-known running-in phase, exhibiting initial friction variations. The second stage, between 14 and 15 minutes, was identified as the stable stage. The last stage, appearing after 20 minutes, was characterized by abrupt friction signal increases. This was ascribed to an accumulation of debris on the scar generating variations in friction. Hence, 20 minutes, achieving a sliding distance of 136 m, was selected for carrying out all the tests.
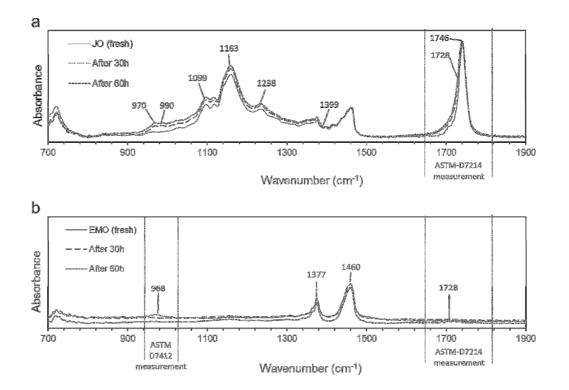
Table 4. Conditions for the reciprocating friction test.

Condition	Values
Oil temperature (°C)	26, 100
Load [N]	20
Contact pressure (GPa)	0.99
Test duration (minutes)	20
Mean sliding distance (m)	136
Reciprocating frequency (Hz)	4.7
Mean sliding velocity (m/s)	0.11
Max. sliding velocity (m/s)	0.22
Stroke length (mm)	12

3   Results and discussion

3.1 Characterization of aged oil samples

The FT-IR spectra from JO, EMO and B20 are shown in Figs. 2a-c, respectively. The spectrum ranges considered for the corresponding ASTM measurements are indicated. The comparison of spectra for fresh and aged JO samples is shown in Fig. 2a. The thermo-oxidation of JO exhibited some characteristic changes. An increase in absorbance in the region between 1650 and 1820 cm^{-1} was identified. It can be related either to the increase in the peak near to 1746 cm^{-1} representing the appearance of saturated aldehyde functional groups or to the formation of other secondary oxidation products that cause absorbance at 1728 cm^{-1} overlapping within the stretching vibration at 1746 cm^{-1} of the ester carbonyl functional group of the triglycerides [32]. A slight increase in the peak near to 1399 cm^{-1} occurred perhaps due to the amount of the oleic acyl groups in the sample [32, 33] or by bending in plane vibrations of CH cis-olefinic groups [32, 34]. The peaks near to 1238 and 1163 cm^{-1} had a growth; which can be attributed to the proportion of saturated acyl groups [32, 33]. The increase in the peak near to 1099 cm^{-1} is commonly presented in oil samples rich in oleic acyl groups [32]. An appearance of the peaks near to 970 and 990 cm^{-1} is evident. It is associated with formation of dimer carboxylic acid [35] that is initially produced by the formation of aldehydes and ketones that then react to form the carboxylic acid and other high-molecular-weight species due to the oxidation process contributing to the polymerization process and viscosity increase. In Fig. 2b, the spectra for fresh and aged EMO samples are compared. Commonly, oxidation of EMOs is represented by an increase in the area between 1650 and 1820 cm^{-1} which is well known as the carbonyl region. The growth of such an area occurs by the absorbance increase in the peak close to 1728 cm^{-1}. For the EMO tested in this work, the increase in the carbonyl region was minimal suggesting low oxidation. However, there was a reduction in the peak near to 968 cm^{-1} suggesting depletion of ZDDP. Also, a diminishment of absorbance in the peaks near to 1377 and 1460 cm^{-1} was found. It can be ascribed to a reduction in the C-H bonds modes of the oil molecules [36]. On the other hand, the spectra shown in Fig. 2c corresponding to B20 exhibited most of the characteristic peaks found in JO and EMO. Moreover, an increase in the peaks near to 1728, 1746, 1238, 1163, 1099, 990 and 970 cm^{-1} was found, akin to that happening in JO. Thus, it can be claimed that the oxidation taking place in B20 overall arises from the oxidation of compounds of JO contained in the blend.
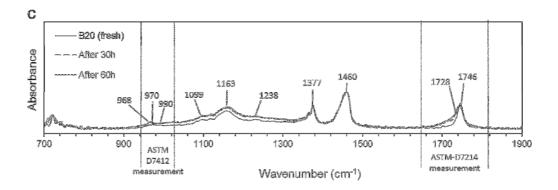
Figure 2. Comparison of FT-IR spectra from fresh and aged oils samples; a) JO; b) EMO; and c) B20.

In Figs. 3a-e, the PAI values, ZDDP concentrations, and changes in viscosity of the oil samples are shown. The PAI values, seen in Fig. 3a, suggest that JO was the most oxidized after the thermo-oxidative process. In contrast, EMO presented very low values, which suggest that it was almost not oxidized. Nevertheless, according to that seen in Fig. 3b, the oxidative process generated reduction of ZDDP concentration in EMO, meaning that they were depleted. On the other hand, B20 exhibited considerable oxidation being attributed to the oxidation of the JO contained in the blend. The results from ZDDP concentration analysis for B20 showed an increase with oxidation time, which would suggest an increase in ZDDP. However, this increase can be ascribed to the formation of dimer carboxylic acid of the JO content in the blend since the measurement region (ASTM D7412) of ZDDP concentration comprises the region of peaks near to 970 and 990 cm^{-1}, as it can be seen in Fig. 2c. So, the measurement of ZDDP for B20 may can be considered as invalid.

According to Figs. 3c-d, the oxidative process generated changes in the viscosity of the three oils at both temperatures. It is well known that the oxidized products and polar components, namely, alcohols, esters, carbonyl compounds and benzene derivatives induce hydrogen bonding, dipole and van der Waals interactions among the constituents present in mineral and synthetic oils contribute to viscosity changes [37]. In a similar way, oxidation in vegetable oils leads to the formation of hydrogen bonds increasing intermolecular forces that increase viscosity [38]. EMO exhibited a slight reduction in viscosity at both temperatures meanwhile B20 and JO showed an increase, with that in JO being the most significant. The decrease in dynamic viscosity of EMO may be attributed to the breaking of hydrocarbons in the oil by high temperatures, forming smaller molecules at an early stage of oxidation [37]. On the other hand, the largest increase of viscosity of JO resulted from the polymerization process produced by the oxidation. It produced the formation of high-molecular weight compounds like those reported for rapeseed oil oxidation [20]. Besides, the formation of hydroperoxides, aldehyde and ketone, as shown in Fig. 2a and 2c, has been demonstrated to be capable of increasing viscosity [35]. The high concentration of saturated acids, namely, araquidic and behenic acids contained in JO, could also produce the viscosity rise [38]. Therefore, the high changes in viscosity of JO due to the thermo-oxidative process suggests its poor oxidative stability. Viscosity changes of JO could be diminished either by adding antioxidant additives or by chemical processes to remove most of saturated acids and other compounds that affect the oxidation stability. In addition, the JO contained in B20 generated a slight increase in viscosity, which can be considered as positive since it may enhance the lubricating properties in specific cases. An increase in viscosity may be considered as helpful to reduce friction and wear in mixed and boundary lubrication conditions occurring in the tribo-system comprised by the piston assembly and cylinder liner. However, a high change in viscosity could be negative for hydrodynamic lubrication situations even for other components in the engine where the viscous shear largely influences the friction force generating larger friction losses and fuel consumption. Also, it may be harmful for the oil pumping in more severe cases. In Fig. 3e, the changes in viscosity index for the different oils can be seen. The fresh JO and EMO samples presented the highest and lowest viscosity index, respectively. Comparing B20 with EMO, fresh B20 presented a higher index than EMO, meaning that JO could enhance

the viscosity index of EMO. However, thermo-oxidation caused a reduction of viscosity index for the three oils, those from JO and B20 were the most affected. A high viscosity index is a signature of high-performance lubricants in most industrial applications where considerable temperature changes are present. The higher the viscosity index values the smaller the viscosity changes or oil thinning with increasing temperature. Hence, fresh JO and B20 presented a better performance, in terms of viscosity index, than EMO but a higher loss of performance by a thermo-oxidative process.
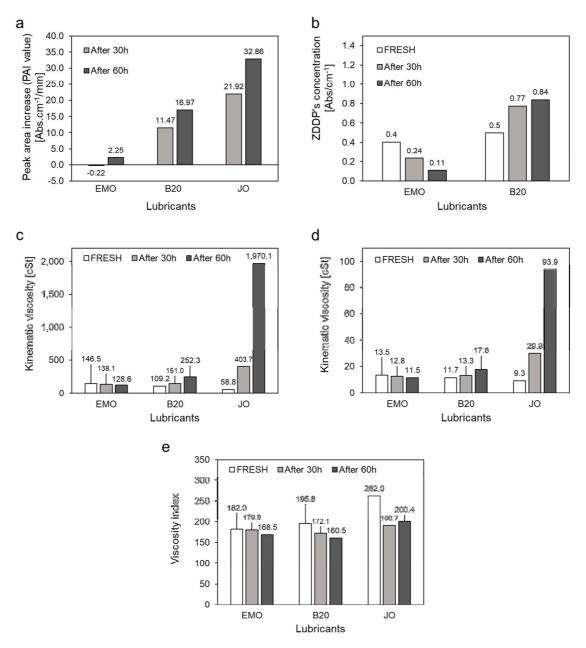

Figure 3. Oxidation and changes in viscosity for the fresh and aged oil samples: a) PAI values; b) ZDDP concentration; c) kinematic viscosities obtained at 26 °C; d) kinematic viscosities obtained at 100 °C; e) viscosity index.

3.2 Tribological behavior

The severity of interaction of asperities at the sliding lubricated interface by using the different oils can be represented by the kind of lubrication regime achieved. It is represented by the Lambda ratio, Λ, which is estimated using an approach outlined previously [39]:

$$\Lambda = \frac{h_{min}}{\sqrt{R_{q1}^2 + R_{q2}^2}} \qquad (1)$$

where, h_{min} is the corresponding minimum film thickness. R_{q1} and R_{q2} are the ball and cylinder liner roughness, respectively. It is considered that the surfaces are separated by a full fluid film (hydrodynamic lubrication regime) at Λ>3. Mixed or partial lubrication occur at 1<Λ<3 meanwhile boundary lubrication is presented at Λ<1 [39]. The minimum film thickness was calculated according to the theory developed by Hamrock et al. [40] for elasto-hydrodynamic lubrication of elliptical conjunctions. Λ value was lower than 0.3 for all the cases, so it can be stated that the whole set of experiments was conducted in the boundary lubrication regime.

According to the evolution of the friction behavior obtained for the fresh and aged lubricant samples at both temperatures, two stages (running-in and stable friction) were identified for all the tests. The first stage covered a period between 3 and 6 minutes where the friction gradually reduced, while in the second the friction remained stable until completion of the 20 minutes of testing. This means that the test conditions used are moving the contact beyond a running-in stage. The friction coefficient reported here corresponds to the average value of the four tests. For this, all the absolute values within the stable friction stage were averaged to obtain a single value for each test. The error bars shown represent the standard deviation of the mean values from the four repetition tests. The comparisons of the mean friction coefficients obtained by using the fresh and aged oils at 26 and 100 ° C are shown in Figs. 4a-b, respectively, meanwhile the wear rates obtained are shown in Figs. 4c-d. Fresh JO and B20 had lower friction coefficients than EMO at both temperatures, which agrees with the behavior reported by other authors [6-11]. It suggests that JO enhanced the EMO´s lubricity properties in a fresh state. The three oils gave an increase in the friction coefficient with oxidation time at 26 °C. JO gave the lowest values while B20 increased friction in a similar manner to EMO. The friction coefficients of JO and B20 increased with ageing time at 100 °C while EMO decreased after 60 h. B20 exhibited the lowest friction coefficient at this temperature. Thus, oxidation of B20 increased the friction coefficients in general, but these were yet lower than those for fresh and aged EMO. The JO contained in B20 promoted low friction coefficients at both temperatures even with oxidation time. It suggests that lubricity of EMO could be improved by blending it with JO even under harsh use conditions.

The standard deviations obtained from the wear rate results were relatively large since the optical profilometer software considered the volume of the scratches made by the surface conditioning (plateau honing) existing in the samples prior to the test. The comparison of wear rates obtained by using the different oils was difficult to establish. Nevertheless, there are some remarkable differences seen in Figs. 4c-d. EMO produced an increase of wear rate with oxidation time at 26 °C, which can be attributed to the ZDDP depletion and the viscosity decrease. On the other hand, JO generated a decrease of wear rate with oxidation time, which can be ascribed to its high increase in viscosity. There was no significant difference in wear rates produced by using fresh and aged B20. The wear rate produced by using fresh JO was higher than that by using EMO at both temperatures. It is ascribed to the difference in viscosity. The wear rates generated by JO at 100 °C had a considerable decrease with oxidation time, which can be ascribed to its large increase in viscosity.
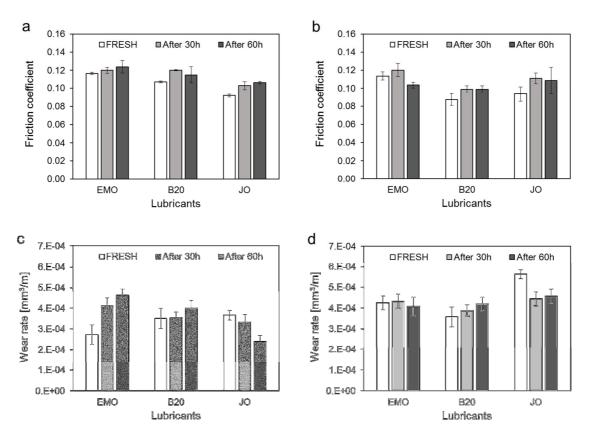
Figure 4. a) Friction coefficients obtained at 26 °C; b) friction coefficients obtained at 100 °C; c) wear rates obtained at 26 °C; b) wear rates obtained at 100 °C.

 An example of the typical wear scars formed can be seen in Figs. 5a-c. In Fig. 5a, an entire scar measured by the optical profilometer is shown. The wear scars generated in the samples were also analyzed by SEM imaging of the surfaces. The typical wear patterns found by SEM are shown in Figs. 5b-c. In Fig. 5b, the representative scar produced by fresh EMO and B20 and aged JO, EMO and B20 at 26 and 100 °C is shown. Mild scuffing wear can be observed in these scars. The only exception was fresh JO tested at 100 °C which generated a scar with different wear (severe scuffing wear), as depicted in Fig. 5c. Both types of wear have been reported to occur in actual cylinder liners under boundary lubrication conditions [41]. They are produced by gradual starvation of the lubricating film under hard loading conditions through sliding of piston rings. Thus, wear is started by the contact and collision between asperities of both ball and cylinder liner surfaces, producing mainly plastic deformation of the asperities of the cylinder liner surface. The asperities are deformed plastically to cover the scratches from the surface finishing (plateau honing), as can be seen in Fig. 5b. This phenomenon, well known as smearing, is the initial stage of the scuffing wear mechanism. The progression of smearing produces surface smoothing forming larger real contact areas. It produces oil film starvation at the contact interface and generates mild adhesion and increase of heat. Mild or severe adhesion can produce detachment of flakes (wear debris) of material from the cylinder liner sample´s surface, as evidenced in Fig. 5c. Those debris are the cause of three-body abrasion that increases the wear rate and alters friction levels. Thus, the severity of wear (severe scuffing) produced by fresh JO at 100 °C could be related to its very low viscosity at this temperature and lack of anti-wear additives (ZDDP), as contained in EMO.
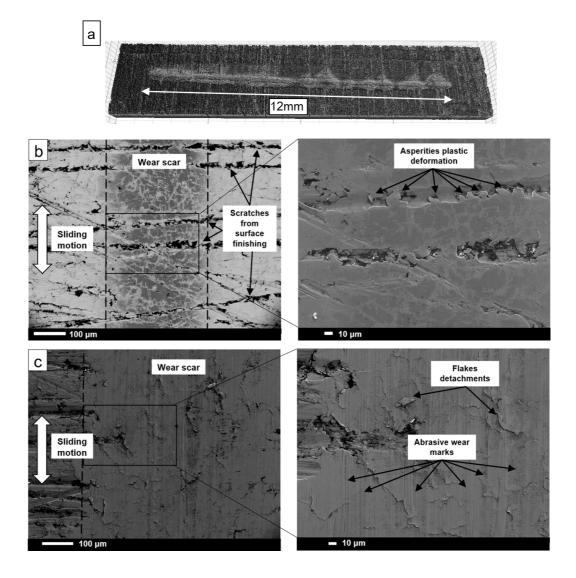
Figure 5. a) Example of an entire wear scar produced in the cylinder liner samples by the reciprocating friction test; b) micrographs from the typical wear scars obtained at 100 °C using fresh EMO exhibiting mild scuffing; c) micrographs from the typical wear scars obtained at 100 °C using fresh JO exhibiting severe scuffing.

Overall, the use of pure JO as engine oil may be harmful because it is highly susceptible to thermo-oxidation, which has been demonstrated to generate considerable physical and chemical changes critical for the engine oil performance. Also, it may be risky for use as engine oil in hydrodynamic lubrication situations, either for the piston assembly or other components in the engine where the viscous shear largely influences the friction force. Oil pumping in the engine could be considerably affected in more severe cases of thermo-oxidation since the observed large viscosity increase in the oil. However, JO may be positively blended with engine mineral oils in low concentrations to enhance lubricity properties without compromising the long-term performance.

4. Conclusions

The effects of thermo-oxidation of Jatropha oil (JO), an engine mineral oil (EMO) and a blend made of 80%vol. EMO and 20%vol. JO (B20) on the tribological behavior of samples from engine cylinder liners by reciprocating friction tests in the boundary lubrication regime at 26 and 100 °C was analyzed in this work. The main conclusions derived from this work are listed below:

- JO exhibited a high increase in viscosity with oxidation time due to polymerization and oxidation of saturated acids, namely, araquidic and behenic acids.
- JO and B20 presented higher viscosity indexes than EMO in fresh state. However, they decreased with oxidation time faster than EMO.
- Thermo-oxidation of JO and B20 increased the friction coefficients, but they were yet lower than those for fresh and oxidized EMO.
- Fresh and oxidized B20 exhibited lower friction coefficients than EMO at both temperatures, suggesting that adding of JO in EMO could be positive to reduce friction even for harsh conditions.
- Fresh JO generated the highest wear rates on the cylinder liner specimens at both temperatures. Nevertheless, the increase in viscosity caused by thermo-oxidation helped to reduce wear.
- Mild and severe scuffing wear patterns were observed on the cylinder liner specimens. Severe scuffing was only seen in those specimens tested by using fresh JO at 100 °C while mild scuffing wear was experienced by the rest of the samples. This was attributed to the lower viscosity of JO and its lack of anti-wear additives as compared with EMO.
- JO could be blended with engine mineral oils in low concentrations to enhance lubricity properties even for long-term use.

Acknowledgements

Funding

References

[1] Holmberg, K., Andersson, P., & Erdemir, A. (2012). Global energy consumption due to friction in passenger cars. Tribology International, 47, 221-234. doi:10.1016/j.triboint.2011.11.022.

[2] Priest, M., & Taylor, C. (2000). Automobile engine tribology — approaching the surface. Wear, 241(2), 193-203. doi:10.1016/s0043-1648(00)00375-6.

[3] Wong, V. W. and Tung S. C. (2016). Overview of Automotive Engine Friction and Reduction Trends–Effects of Surface, Material, and Lubricant-Additive Technologies. Friction, 4(1), 1–28. doi:10.1007/s40544-016-0107-9.

[4] Mohamed, E. S. (2018). Performance Analysis and Condition Monitoring of ICE Piston-Ring Based on Combustion and Thermal Characteristics. Applied Thermal Engineering, 132, 824–840. doi:10.1016/j.applthermaleng.2017.12.111.

[5] Tung, S. C. & Hartfield W. S. (1995). Advanced engine materials: current development and future trends, in NIST (National Inst. of Science and Technology), Engine Materials and Tribology Workshop, Gaithersburg, MD, April 4-7, 1995.

[6] Fox, N., Tyrer, B., & Stachowiak, G. (2004). Boundary Lubrication Performance of Free Fatty Acids in Sunflower Oil. Tribology Letters, 16(4), 275-281. doi:10.1023/b:tril.0000015203.08570.82.

[7] Chatra, K. R. S., Jayadas, N. H., and Kailas, S. V. (2012). Chapter 11: Natural oil-based lubricants, in Green Tribology, Green Energy and Technology, Bangalore, India, Springer-Verlag Berlin Heidelberg.

[8] Nagendramma, P., & Kaul, S. (2012). Development of ecofriendly/biodegradable lubricants: An overview. Renewable and Sustainable Energy Reviews, 16(1), 764-774. doi:10.1016/j.rser.2011.09.002.

[9] Bahari, A., Lewis, R., & Slatter, T. (2017). Friction and wear response of vegetable oils and their blends with mineral engine oil in a reciprocating sliding contact at severe contact conditions. Proceedings of the Institution of Mechanical Engineers, Part J: Journal of Engineering Tribology, 1-15. doi:10.1177/1350650117712344.

[10] Ruggiero, A., D'Amato, R., Merola, M., Valašek, P., & Müller, M. (2017). Tribological characterization of vegetal lubricants: Comparative experimental investigation on Jatropha curcas L. oil, Rapeseed Methyl Ester oil, Hydrotreated Rapeseed oil. Tribology International, 109, 529-540. doi:10.1016/j.triboint.2017.01.030.

[11] Mobarak, H., Mohamad, E. N., Masjuki, H., Kalam, M., Mahmud, K. A., Habibullah, M., & Ashraful, A. (2014). The prospects of biolubricants as alternatives in automotive applications. Renewable and Sustainable Energy Reviews, 33, 34-43. doi:10.1016/j.rser.2014.01.062.

[12] Alves, S., Barros, B., Trajano, M., Ribeiro, K., & Moura, E. (2013). Tribological behavior of vegetable oil-based lubricants with nanoparticles of oxides in boundary lubrication conditions. Tribology International, 65, 28-36. doi:10.1016/j.triboint.2013.03.027.

[13] Quinchia, L., Delgado, M., Reddyhoff, T., Gallegos, C., & Spikes, H. (2014). Tribological studies of potential vegetable oil-based lubricants containing environmentally friendly viscosity modifiers. Tribology International, 69, 110-117. doi:10.1016/j.triboint.2013.08.016.

[14] Shahabuddin, M., Masjuki, H., Kalam, M., Bhuiya, M., & Mehat, H. (2013). Comparative tribological investigation of bio-lubricant formulated from a non-edible oil source (Jatropha oil). Industrial Crops and Products, 47, 323-330. doi:10.1016/j.indcrop.2013.03.026.

[15] Shahabuddin, M., Masjuki, H., & Kalam, M. (2013). Experimental Investigation into Tribological Characteristics of Bio-Lubricant Formulated from Jatropha Oil. Procedia Engineering, 56, 597-606. doi:10.1016/j.proeng.2013.03.165.

[16] Vipper, A. B., Zadko, I. I., Ermolaev, M. V., & Oleinik, J. Y. (2002). Engine oil ageing under laboratory conditions. Lubrication Science, 14(3), 363-375. doi:10.1002/ls.3010140307.

[17] Fox, N., & Stachowiak, G. (2007). Vegetable oil-based lubricants—A review of oxidation. Tribology International, 40(7), 1035-1046. doi:10.1016/j.triboint.2006.10.001.

[18] Zainal, N., Zulkifli, N., Gulzar, M., & Masjuki, H. (2018). A review on the chemistry, production, and technological potential of bio-based lubricants. Renewable and Sustainable Energy Reviews, 82, 80-102. doi:10.1016/j.rser.2017.09.004.

[19] Mannekote, J. K., & Kailas, S. V. (2012). The Effect of Oxidation on the Tribological Performance of Few Vegetable Oils. Journal of Materials Research and Technology, 1(2), 91-95. doi:10.1016/s2238-7854(12)70017-0.

[20] Kreivaitis, R., Padgurskas, J., Gumbytė, M., Makarevičienė, V., & Spruogis, B. (2011). The influence of Oxidation on Tribological Properties of Rapeseed Oil. Transport, 26(2), 121-127. doi:10.3846/16484142.2011.586109.

[21] Martinez, H. J. (2007). The mexican jatropha seed: a bioenergetic alternative for Mexico. Revista Digital Universitaria, 8(12), 2007, http://www.revista.unam.mx/vol.8/num12/art88/int88.htm.

[22] Farfan-Cabrera, L. I., Gallardo-Hernández, E. A., & Pérez-González, J. (2017). Compatibility study of common sealing elastomers with a biolubricant (Jatropha oil). Tribology International, 116, 1-8. doi:10.1016/j.triboint.2017.06.039.

[23] Farfan-Cabrera, L. I., Gallardo-Hernández, E. A., Reséndiz-Calderón, C. D., & Rosa, C. S. (2018). Physical and Tribological Properties Degradation of Silicone Rubber Using Jatropha Biolubricant. Tribology Transactions, 61(4), 640-647.

[24] Farfan-Cabrera, L. I., Pérez-González, J., & Gallardo-Hernández, E. A. (2018). Deterioration of seals of automotive fuel systems upon exposure to straight Jatropha oil and diesel. Renewable Energy, 127, 125-133. doi:10.1016/j.renene.2018.04.048.

[25] Golshokouh, I., Syahrullail, S., Shariatmadari, S., & Ani, F. N. (2013). Investigate Jatropha Oil as New Source of Lubricant Oil. Applied Mechanics and Materials, 465-466, 201-205. doi:10.4028/www.scientific.net/amm.465-466.201.

[26] Shashidhara, Y., & Jayaram, S. (2010). Vegetable oils as a potential cutting fluid—An evolution. Tribology International, 43(5-6), 1073-1081. doi:10.1016/j.triboint.2009.12.065.

[27] Talib, N., & Rahim, E. (2015). Performance Evaluation of Chemically Modified Crude Jatropha Oil as a Bio-based Metalworking Fluids for Machining Process. Procedia CIRP, 26, 346-350. doi:10.1016/j.procir.2014.07.155.

[28] Farfan-Cabrera, L. I., Gallardo-Hernández, E. A., Vite-Torres, M., & Laguna-Camacho, J. R. (2015). Frictional Behavior of a Wet Clutch Using Blends of Automatic Transmission Fluid (ATF) and Biolubricant (JatrophaOil) in a Pin-on-Disk Tester. Tribology Transactions, 58(5), 941-946. doi:10.1080/10402004.2015.1032461.

[29] Paswan, B. K., Jain, R., Sharma, S. K., Mahto, V., Sharma, V. P. (2016). Development of Jatropha oil-in-water emulsion drilling mud system. Journal of Petroleum Science and Engineering, 144, 10-18. http://dx.doi.org/10.1016/j.petrol.2016.03.002.

[30] Besser, C., Schneidhofer, C., Dörr, N., Novotny-Farkas, F., & Allmaier, G. (2012). Investigation of long-term engine oil performance using lab-based artificial ageing illustrated by the impact of ethanol as fuel component. Tribology International, 46(1), 174-182. doi:10.1016/j.triboint.2011.06.026.

[31] Johnson, K. L. (2004). Contact mechanics. Cambridge: Cambridge University Press.

[32] Liang, P., Chen, C., Zhao, S., Ge, F., Liu, D., Liu, B., Fan, Q., Han, B., Xiong, X. (2013). Application of Fourier Transform Infrared Spectroscopy for the Oxidation and Peroxide Value Evaluation in Virgin Walnut Oil. Journal of Spectroscopy, 2013, 1-5. doi:10.1155/2013/138728.

[33] Guillén, M. D., & Cabo, N. (1997). Characterization of edible oils and lard by fourier transform infrared spectroscopy. Relationships between composition and frequency of concrete bands in the fingerprint region. Journal of the American Oil Chemists Society, 74(10), 1281-1286. doi:10.1007/s11746-997-0058-4.

[34] Dahlberg, D. B., Lee, S. M., Wenger, S. J., & Vargo, J. A. (1997). Classification of Vegetable Oils by FT-IR. Applied Spectroscopy, 51(8), 1118-1124. doi:10.1366/0003702971941935.

[35] Lubis, A. M., Ariwahjoedi, B., & Sudin, M. B. (2015). Investigation on oxidation of jatropha oil. Proceedings of Mechanical Engineering Research Day, 2015, 53-54.

[36] Uy, D., Zdrodowski, R. J., Oneill, A. E., Simko, S. J., Gangopadhyay, A. K., Morcos, M., Lauterwasser, F., Parsons, G. (2011). Comparison of the Effects of Biodiesel and Mineral Diesel Fuel Dilution on Aged Engine Oil Properties. Tribology Transactions, 54(5), 749-763. doi:10.1080/10402004.2011.597545.

[37] Tripathi, A., & Vinu, R. (2015). Characterization of Thermal Stability of Synthetic and Semi-Synthetic Engine Oils. Lubricants, 3(1), 54-79. doi:10.3390/lubricants3010054.

[38] Sathianathan, R. V., Kannapiran, A., Govindan, J., & Periasamy, N. (2014). Profiling of Fatty Acid Compositional Alterations in Edible Oils Upon Heating Using Gas Chromatography. Journal of Physical Science, 25(2), 1-14.

[39] Hutchings, I. (1992). Tribology: friction and wear of engineering materials (First ed.). S.l.: Elsevier Butterworth-Hein.

[40] Hamrock, B. J., Schmid, S. R., & Jacobson, B. O. (2004). Fundamentals of fluid film lubrication. New York: Marcel Dekker.

[41] Jensen, M. F., Bøttiger, J., Reitz, H. H., & Benzon, M. E. (2002). Simulation of wear characteristics of engine cylinders. Wear, 253(9-10), 1044-1056. doi:10.1016/s0043-1648(02)00251-x.